Pancholi and K. Way, *ibid.* B2 (No. 6), 1 (1968); $A=67$: S. C. Pancholi and W. B. Ewbank, *ibid.* B2 (No. 6), 71 (1968).
[24]S. Cohen, R. D. Lawson, M. H. Macfarlane, S. P. Pandya, and M. Soga, Phys. Rev. 160, 903 (1967).
[25]N. Auerbach, Phys. Rev. 163, 1203 (1967).
[26]E. A. Phillips and A. D. Jackson, Phys. Rev. 169, 917 (1968).
[27]^{58}Cu: J. A. Cookson, Phys. Letters 24B, 570 (1967); ^{60}Cu: H. J. Young and J. Rapaport, *ibid.* 26B, 143 (1968); ^{62}Cu, the present work; ^{64}Cu: W. T. Bass and P. H. Stelson, Phys. Rev. C 2, 2154 (1970); ^{66}Cu: W. W. Daehnick and Y. S. Park, Phys. Rev. 180, 1062 (1969); ^{68}Cu: H. Bakhru and S. K. Mukherjee, Nucl. Phys. 52, 125 (1964).
[28]L. G. Mann, K. G. Tirsell, and S. D. Bloom, Nucl. Phys. A97, 425 (1967).

PHYSICAL REVIEW C VOLUME 7, NUMBER 2 FEBRUARY 1973

Spin-Orbit and Target Spin Effects in Helion Elastic Scattering*

C. B. Fulmer and J. C. Hafele†
Oak Ridge National Laboratory, Oak Ridge, Tennessee 37830
(Received 28 August 1972)

The well depth of the spin-orbit term for the helion-nucleus optical-model potential was determined by performing parameter searches for elastic scattering data at successive fixed values of V_s. Resulting plots of χ^2/N vs V_s show consistent minima for the 13 data sets used. Elastic angular distributions studied were for ^{60}Ni at four energies between 35 and 71 MeV and for three groups of neighboring even- and odd-mass targets at energies between 60 and 71 MeV. The χ^2/N vs V_s plots for all the even-mass ($I=0$) targets have minima at values of V_s between 2.0 and 3.0 MeV, while the plots for all the odd-mass ($I\neq 0$) targets have minima about 1 MeV greater (3.0 to 4.0 MeV). This difference in the best-fit values of V_s is consistent over a wide range of target mass and of scattering energy, and suggests the presence of a detectable target spin interaction in helion elastic scattering.

I. INTRODUCTION

The well established need for a spin-orbit term in the nucleon-nucleus optical-model potential suggests the use of a similar term in the helion-nucleus optical potential. Although theoretical estimates[1,2] predict a spin-orbit well depth between 2 and 3 MeV for helions, previous attempts[3-5] to measure the strength of this interaction have suffered from serious ambiguities. Hodgson[3] has pointed out that it is unwise to attempt to deduce the depth of the spin-orbit term from mere improvement of fits to one or two angular distributions, and that one should look for a consistent effect in fits to a large number of data sets. This is true because inclusion of the spin-orbit term usually produces only minor improvement. In fact many previous optical-model analyses of helion elastic scattering have ignored it altogether.

When experimental angular distributions for scattering at intermediate energies extend into the backward hemisphere, however, significantly improved fits occur when the spin-orbit term is included in the potential. In a previous study of the elastic scattering of 59.8-MeV helions from ^{27}Al, we observed that a spin-orbit well depth of about 2.3 MeV is definitely indicated when large-angle data were included in the data set.[6] When the data set was reduced to contain only the data for angles forward of about 70°, however, satisfactory fits were obtained with no spin-orbit term.[6] These results suggest that both high-energy and large-angle data are required.

In addition to the projectile spin-orbit interaction, a similar but somewhat weaker interaction proportional to the spin and orbital angular momentum of the target nucleus is expected.[7] Preliminary evidence for such a term in the optical potential for helion elastic scattering has been reported.[8] More extensive evidence, however, is clearly desirable.

We report here the results of a study of the systematic effect of the spin-orbit term on optical-model fits to 13 angular distributions for helion elastic scattering from targets of a wide range of mass and for energies between 35 and 71 MeV.

II. DATA AND ANALYSIS

The targets, scattering energies, and angular ranges of the data sets used are listed in Table I.

The 35-MeV data for ^{60}Ni and ^{59}Co are from the work of Leutzelschwab and Hafele,[9] and the rest of the data sets were obtained at the Oak Ridge Isochronous Cyclotron Laboratory. All the data sets extend to angles $\geq 110°$.

Optical-model calculations were done with the automatic search code GENOA.[10] The optical potential consisted of a conventional Woods-Saxon real term (well depth V), a derivative Woods-Saxon surface imaginary term (well depth W_D), and a term for the Coulomb potential of a uniformly charged sphere of radius $1.3A^{1/3}$ fm. The spin-orbit term (well depth V_s) was of the usual form proportional to $\vec{\sigma}\cdot\vec{l}$, where $\vec{\sigma}$ is the projectile spin and $\vec{l}$ the barycentric orbital angular momentum. As was the case in the analysis of Ref. 6, the radius parameter for the spin-orbit term (r_s) was set equal to that for the real term (r_R), and the diffuseness parameters for these terms were also equated ($a_s = a_R$). Surface absorption was used exclusively because it appears to produce fits superior to those obtained with volume absorption.[6] We denote the number of data points in a data set by N, and χ^2/N is the usual (normalized) goodness-of-fit criterion.

The purpose of this study was to search for a systematic behavior for the spin-dependent part of the optical potential, with both even- and odd-mass (zero- and nonzero-spin) targets. Although the GENOA code did not permit introduction of a term representing a target spin-orbit interaction proportional to $\vec{I}\cdot\vec{l}$, or one representing a spin-spin interaction proportional to $\vec{I}\cdot\vec{\sigma}$ (I is the target nuclear spin), we found that the data for the targets with $I \neq 0$ could be fitted satisfactorily with the projectile spin-orbit term alone. Because the effect of a target spin-dependent interaction on elastic scattering angular distributions is expected to be similar to that for the projectile spin-orbit interaction, the presence of a detectable target spin interaction should be apparent in the optical-model analyses as somewhat greater values of V_s for the odd-mass targets than those for neighboring even-mass targets. Although this approach produced consistent results, it is desirable to repeat some of these calculations with an appropriate target spin term in the potential.

For each data set a fixed value was assigned to V_s, and χ^2/N was minimized by permitting the code to vary the other parameters. Then V_s was incremented by 1 MeV and the parameter search was repeated. The results of these searches yielded a plot of minimum values of χ^2/N vs V_s for each data set. In some cases, fixed values were assigned to the well depths V and W_D; in these cases the assigned values were determined from results of a previous study of helion scattering from ^{60}Ni at several bombarding energies.[11] In other cases searches were performed with V and W_D as variable parameters.

TABLE I. Helion elastic scattering angular distributions used in V_s-gridding studies. The energy values are the laboratory energies of the incident beams after traversing half the target foil thickness. The last six columns are the parameters obtained for the minimum values of χ^2/N vs V_s. Underlined parameter values were not varied in the searches.

	Data sets		Optical-model parameters					
Target	Energy (MeV)	Angular range (deg)	V (MeV)	$r_R = r_s$ (fm)	$a_R = a_s$ (fm)	W_D (MeV)	r_I (fm)	a_I (fm)
^{51}V	59.8	18–112	128	1.10	0.818	20.5	1.25	0.774
^{51}V	59.8	18–112	140	1.00	0.872	19.8	1.25	0.802
^{52}Cr	59.8	18–149	128	1.09	0.824	20.5	1.23	0.805
^{52}Cr	59.8	18–149	132	1.06	0.847	20.5	1.23	0.804
^{53}Cr	59.8	29–112	128	1.10	0.823	20.5	1.27	0.762
^{53}Cr	59.8	29–112	130	1.09	0.830	20.2	1.27	0.770
^{59}Co	59.8	20–112	125	1.13	0.792	20.5	1.28	0.754
^{59}Co	49.7	15–128	126	1.12	0.848	20.5	1.28	0.803
^{59}Co	34.8	7–142	128	1.14	0.772	20.5	1.24	0.877
^{60}Ni	71.1	19–109	123	1.12	0.837	20.5	1.24	0.828
^{60}Ni	59.8	18–112	125	1.12	0.816	20.5	1.24	0.828
^{60}Ni	49.7	14–128	126	1.13	0.842	20.5	1.26	0.835
^{60}Ni	35.1	7–152	128	1.14	0.768	20.5	1.21	0.882
^{144}Sm	59.8	23–111	110	1.10	0.960	22.0	1.27	0.840
^{208}Pb	71.1	18–117	123	1.11	0.736	24.4	1.07	0.972
^{209}Bi	71.1	18–117	132	1.06	0.776	25.1	1.06	0.949

TABLE II. Values of optical-model parameters obtained in V_s-grid searches on 59.8-MeV data from ^{53}Cr. Underlined parameter values were not varied in the searches. The χ^2/N vs V_s plot obtained with V and W_D variable is very similar to the plot obtained with V and W_D fixed at 128 and 20.5 MeV, respectively. The latter plot is shown in Fig. 3.

V_s (MeV)	V (MeV)	$r_R = r_s$ (fm)	$a_R = a_s$ (fm)	W_D (MeV)	r_I (fm)	a_I (fm)
0	109	1.20	0.751	19.7	1.27	0.771
1	112	1.18	0.766	19.8	1.27	0.771
2	117	1.16	0.782	20.0	1.27	0.762
3	127	1.10	0.816	20.2	1.27	0.765
4	143	1.02	0.873	20.5	1.26	0.774
5	160	0.920	0.928	20.7	1.25	0.792
0	128	1.10	0.821	20.5	1.28	0.754
1	128	1.10	0.816	20.5	1.28	0.754
2	128	1.10	0.818	20.5	1.28	0.751
3	128	1.10	0.821	20.5	1.27	0.757
4	128	1.09	0.825	20.5	1.26	0.766
5	128	1.08	0.839	20.5	1.23	0.795

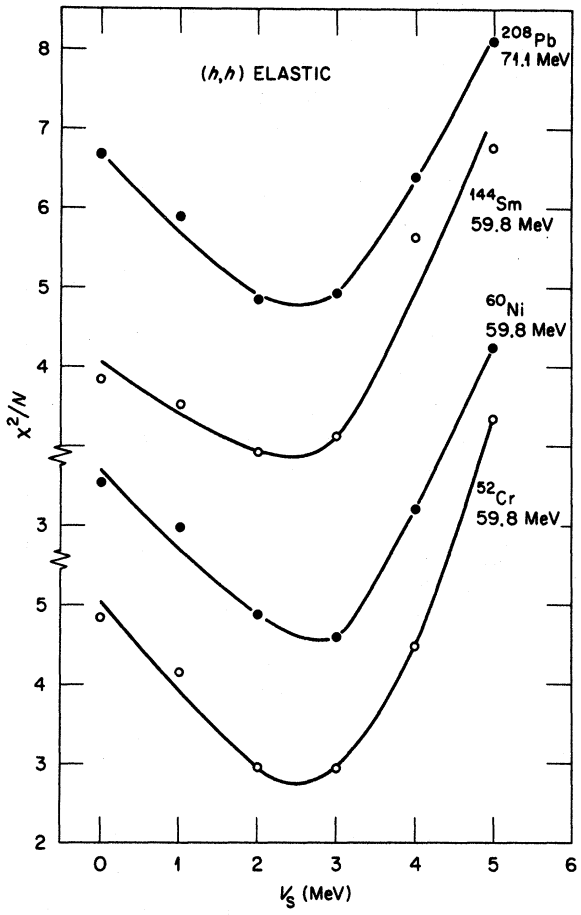

FIG. 1. χ^2/N vs V_s for helion elastic scattering from $I=0$ targets. Angular ranges of the data and optical-model parameters at the minima are listed in Table I.

III. RESULTS AND DISCUSSION

The values of the potential parameters at the minima of the resulting plots of χ^2/N vs V_s are listed in Table I. In all cases V lies between 120 and 132 MeV, except for ^{144}Sm and for ^{51}V with variable V. In this latter case, $r_R = 1.00$ fm, which is exceptionally low compared with the average near 1.10 fm, and is probably associated with the well known continuous $V(r_R)^n$ ambiguity. Also notable in Table I is a near constancy of the geometrical and depth parameters for the absorption

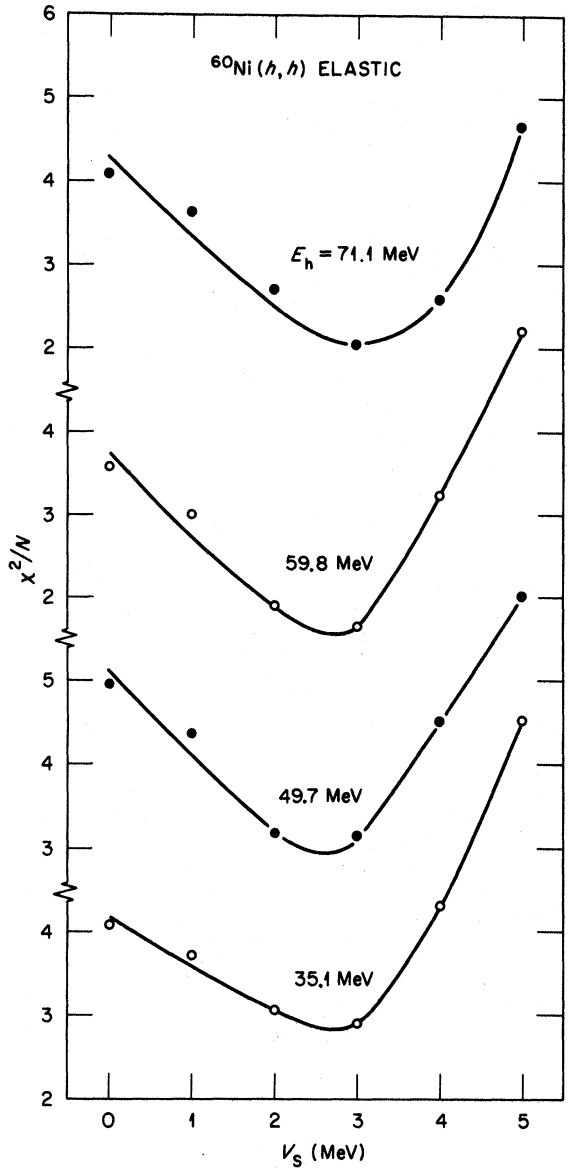

FIG. 2. χ^2/N vs V_s for helion elastic scattering from ^{60}Ni at several incident particle energies. Angular ranges of the data and optical-model parameters at the minima are listed in Table I.

potential. The greatest deviations of these parameters from average values occur for ^{208}Pb and ^{209}Bi, where r_I is somewhat smaller and a_I somewhat larger than for the lower-mass cases.

Table II lists the values of the potential parameters obtained from each of the V_s = constant searches for the ^{53}Cr data set. The values in this case illustrate the trends observed with all the other data sets. An obvious trend when V is variable is an increase in V with decreasing r_R, which indicates the presence of the $V(r_R)^n$ ambiguity. Also notable is an increase in V with increasing V_s, and a corresponding increase in a_R. However, when W_D is variable, the values obtained change very little over the range of values of V_s used. We also observe only small changes in r_I and a_I, whether W_D is variable or not. The results of Ref. 6 suggest that if data for larger angles had been included in the data sets, the $V(r_R)^n$ ambiguity would have been significantly suppressed.

Figures 1 and 2 show the plots of χ^2/N vs V_s for the even-mass ($I=0$) targets. For these figures and the other figures in this paper, smooth curves have been drawn through the plotted points to guide the eye. Figure 1 shows that the minimum values of V_s are remarkably constant for a wide range of target masses. The plots in Fig. 2 for ^{60}Ni illustrate the same effect with a fixed

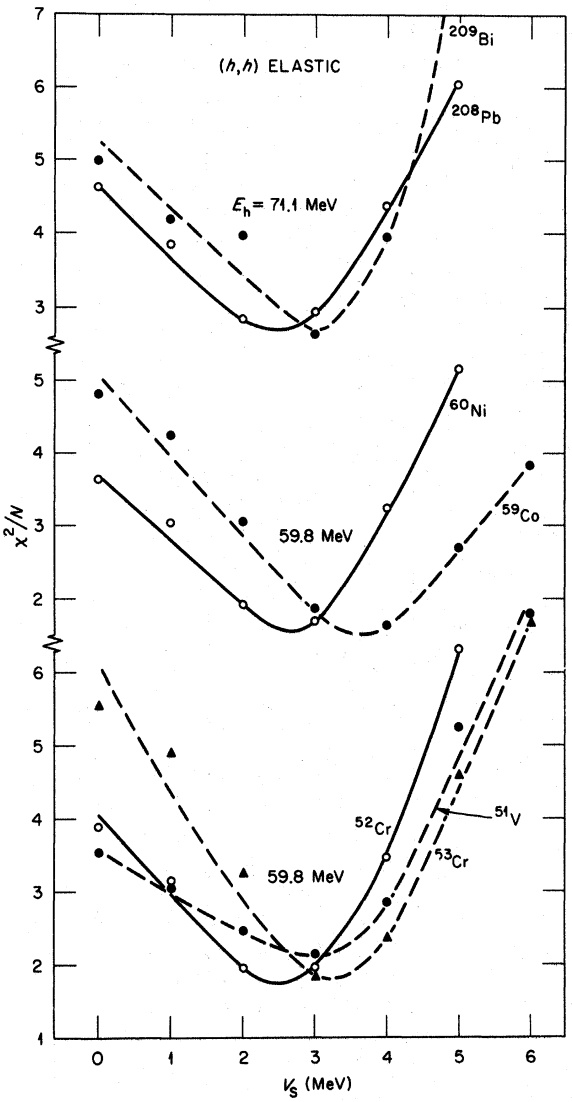

FIG. 3. χ^2/N vs V_s for helion elastic scattering from targets of neighboring mass with and without target spin. Angular ranges of the data and optical-model parameters at the minima are listed in Table I.

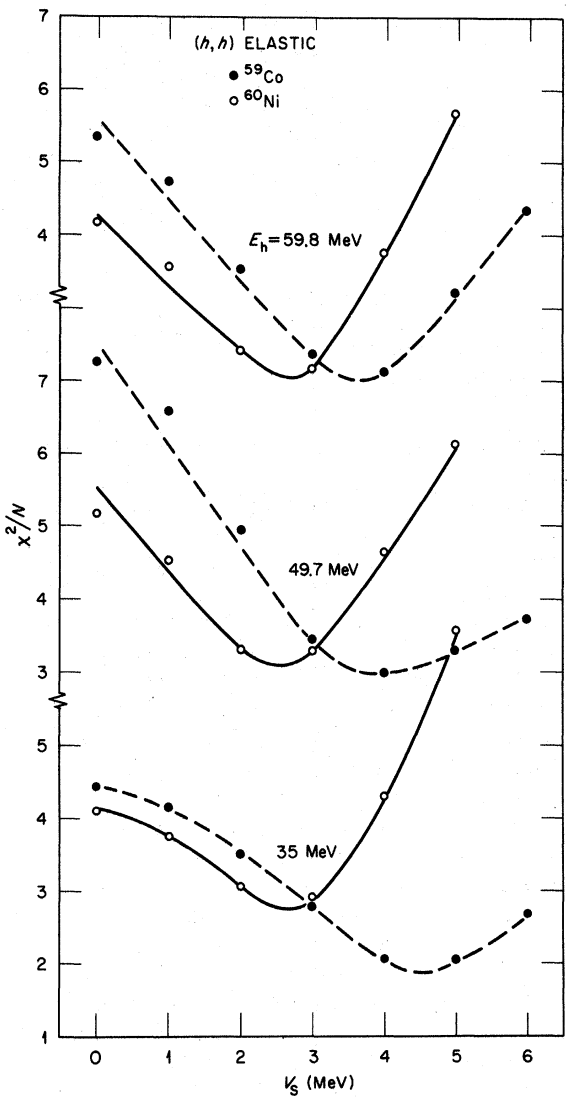

FIG. 4. χ^2/N vs V_s for helion elastic scattering from ^{59}Co($I=\frac{7}{2}$) and ^{60}Ni($I=0$). Angular ranges of the data and optical-model parameters at the minima are listed in Table I.

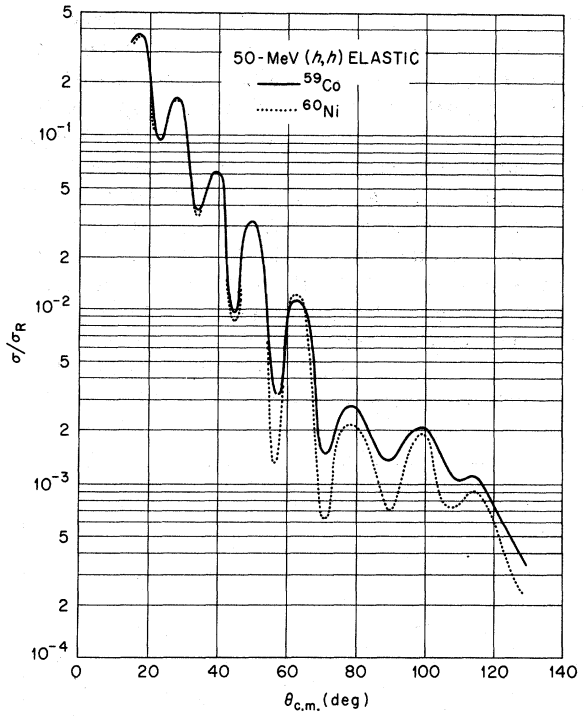

FIG. 5. Angular distributions for 50-MeV helion elastic scattering from ^{59}Co and ^{60}Ni. The plot for each target was obtained by drawing a smooth curve through the experimental data.

target mass and for a wide range of scattering energies.

The minima for all the curves in Figs. 1 and 2 occur at values of V_s between 2.0 and 3.0 MeV. Although the minima in these curves are not particularly sharp and well defined, an important feature is their consistency. The broad and shallow nature of these minima is the primary reason why V_s was poorly defined in most previous studies, for any of these curves alone would not be particularly decisive. These consistent results for a large number of data sets, however, are reasonably strong evidence that the depth of the spin-orbit term in the helion-nucleus potential for spin-zero targets is 2.0 to 3.0 MeV. They also suggest that V_s is fairly independent of target mass and of scattering energy. Although these results generally agree with results of previous studies, this is the first time to our knowledge that V_s has been defined in such a consistent manner.

The minimum value of V_s is least well defined for the case of ^{60}Ni at 35.1 MeV. Figure 2 shows the somewhat broader minimum that occurs in this case, even though the angular range of this data set is the largest of those studied. This demonstrates the importance of higher energies for better definition of V_s as was concluded in a recent extensive analysis of 33-MeV data by Cage *et al.*[12]

The same procedures applied to the data sets for the odd-mass ($I \neq 0$) targets produced another interesting result. Figure 3 shows plots of χ^2/N vs V_s for three groups of neighboring even-odd-mass targets. In all groups the minima for the targets with $I \neq 0$ occur at larger values of V_s than those for the targets with $I = 0$. Figure 4 shows the same effect for a fixed target pair and a wide range of scattering energies. In each case in Fig. 4, the minimum for ^{59}Co occurs at a larger value of V_s than that for ^{60}Ni. These figures show that, over a wide range of target mass and scattering energy, the odd-mass targets have minima at values of V_s between 3.0 and 4.0 MeV (except for ^{59}Co at 35 MeV), or about 1.0 MeV greater than the values for the even-mass targets. Because the nuclear spins for the odd-mass targets cover a large range of values, it also appears that the magnitude of this enhancement of V_s is fairly independent of the actual value of the target nuclear spin provided it is not zero.

To illustrate typical differences observed in angular distributions for neighboring even-odd-mass targets, the measured angular distributions for ^{59}Co and ^{60}Ni at 50 MeV are compared in Fig. 5. This figure shows smooth curves drawn through the original data points. In Ref. 8, where these data were first reported, the pronounced differences for angles greater than about 70° were interpreted as evidence for a dependence of helion elastic scattering on target spin, but the evidence was weak because only one case was available. The results shown in Figs. 3 and 4 corroborate and strengthen this earlier conclusion. Again the strength of the evidence is not the sharpness of the minima, but rather the consistency of the minima over a wide range of target mass and scattering energy.

In contrast with these results for helions, significant target spin effects have not been observed in studies of elastic scattering of nucleons from nuclei. Measured polarization angular distributions for protons scattered from ^{24}Mg ($I = 0$) and from ^{27}Al ($I = \frac{5}{2}$) at similar energies (~11 MeV) are almost identical.[13] Furthermore, angular distributions covering a large range of angles for 40-MeV protons elastically scattered from ^{58}Ni ($I = 0$), ^{59}Co ($I = \frac{7}{2}$), and ^{60}Ni ($I = 0$) are indistinguishable.[14] However, anomalous s-wave strength functions for neutrons have been explained by Seth as being due to a spin-spin interaction.[15] It is probable that target spin effects are present in the nucleon-nucleus interaction, but if this is the case they are too weak to be apparent in elastic angular dis-

tributions with typical errors. Perhaps a 10-fold or more reduction in experimental errors would permit detection of even-odd-mass differences in proton elastic scattering angular distributions.

In the case of the α-nucleus optical potential, the projectile spin-orbit term vanishes because the projectile is spinless, and the only nonzero spin that may be present is the target nuclear spin. Taylor, Fletcher, and Davis[16] observed the need for a target spin-orbit term in an optical-model analysis of elastic scattering of α particles from ^{9}Be. We have also measured elastic cross sections for 50-MeV α particles scattered from ^{59}Co and ^{60}Ni, and found significant large-angle differences[17] similar to those shown in Fig. 5. More recently Weller[18] has reported evidence for an $\vec{I}\cdot\vec{I}$ dependence in the level spacing for α-particle bound states. Thus it appears that target spin effects are readily apparent in both helion and α interactions.

Perhaps the absence of target spin effects in proton scattering studies is related to the much weaker absorption of protons in nuclear matter. For comparable target mass and scattering energy, typical backward-angle elastic cross sections are several orders of magnitude greater for protons than they are for helions and α particles. This suggests that protons are scattered more uniformly throughout the target nuclear volume, while the strong absorption of helions and α particles confines their scattering to the surface region. Because the wave functions for valence nucleons generally peak near the nuclear surface, the spin-contributing nucleons are expected to be concentrated in the nuclear surface, and projectiles primarily scattered in the surface region should therefore be more strongly influenced by target spin. Although protons are certainly scattered by the valence nucleons, a much larger contribution probably comes from the nuclear interior, which tends to mask any dependence of the interaction on target spin. An optical-model code with a target spin-orbit term would be very useful in a detailed study of these ideas.

As was noted above, the strength of the target spin dependence in helion scattering does not appear to be strongly dependent on the actual value of I, providing only that $I \neq 0$. In every case of an odd-mass target in Figs. 3 and 4 (except for ^{59}Co at 35 MeV), the minima in the plots of χ^2/N vs V_s lie consistently between 3.0 and 4.0 MeV, even though the target spins range between $\frac{3}{2}$ and $\frac{9}{2}$. This observation agrees with one of the main predictions of a recent theoretical study by Rawitscher,[19] who showed that the depth of the target spin-orbit term in the α-nucleus optical potential should be very weakly dependent on I, provided $I \neq 0$. These results are in strong contrast, however, with a target spin dependence previously expected to be inversely proportional to the target mass (A^{-1} dependence).[20] Furthermore, the relative role played by a spin-spin interaction is not clear at this time. Additional work in this area will probably reveal more detailed information about these target spin interactions.

In conclusion, the study reported in this paper shows the need for a target spin term as well as a projectile spin-orbit term in the optical-model potential for helion-nucleus scattering. Both of these terms appear to have a weak dependence on target mass and scattering energy. In addition, the target spin term has a weak dependence on the actual value of the target nuclear spin if it is nonzero.

IV. ACKNOWLEDGMENTS

We acknowledge the superb performance of the Oak Ridge isochronous cyclotron operating crew during the data acquisition phase of this work. We also thank F. G. Perey for providing the optical-model code GENOA. The support of Oak Ridge Associated Universities is also gratefully acknowledged.

---

*Research sponsored by the U. S. Atomic Energy Commission under contract with Union Carbide Corporation.

†1969 and 1970 Oak Ridge Associated Universities summer research participant from Washington University, St. Louis, Missouri. Present address: Research Department, Caterpillar Tractor Company, Peoria, Illinois 61602.

[1]C. R. Bingham and M. L. Halbert, Phys. Rev. 169, 933 (1968).

[2]A. Y. Abul. Magd and M. El-Nadi, Progr. Theoret. Phys. (Kyoto) 35, 788 (1966).

[3]R. E. Hodgson, Advan. Phys. 17, 202 (1968).

[4]G. R. Siegel, Ph.D. thesis, Washington University, St. Louis, Missouri, 1971 (unpublished).

[5]J. B. A. England, R. G. Harris, L. H. Watson, and D. H. Worledge, Nucl. Phys. A165, 277 (1971).

[6]C. B. Fulmer and J. C. Hafele, Phys. Rev. C 5, 1969 (1972); and Bull. Am. Phys. Soc. 16, 99 (1971).

[7]H. Feshbach, in *Nuclear Spectroscopy*, edited by F. Ajzenberg-Selove (Academic, New York, 1960), Pt. B.

[8]J. C. Hafele, C. B. Fulmer, and F. G. Kingston, Phys. Letters 31, 17 (1970).

[9]J. W. Leutzelschwab and J. C. Hafele, Phys. Rev. 180, 1023 (1969).

[10]F. G. Perey, unpublished.
[11]C. B. Fulmer, J. C. Hafele, and C. C. Foster, Bull. Am. Phys. Soc. 16, 1165 (1971); and to be published.
[12]M. E. Cage, D. L. Clough, A. J. Cole, J. B. A. England, G. J. Pyle, P. M. Rolph, L. H. Watson, and D. H. Worledge, Nucl. Phys. A183, 449 (1972).
[13]L. Rosen, in *Proceedings of the International Conference on Nuclear Structure, Kingston, 1960,* edited by D. A. Bromley and E.W. Vogt (Univ. of Toronto Press, Toronto, Canada, 1960), p. 185.
[14]M. P. Fricke, E. E. Gross, B. J. Morton, and A. Zucker, Phys. Rev. 156, 1207 (1967).
[15]K. K. Seth, Nucl. Phys. 24, 169 (1961).
[16]R. B. Taylor, N. R. Fletcher, and R. H. Davis, Nucl. Phys. 65, 318 (1965).
[17]C. B. Fulmer and J. C. Hafele, Bull. Am. Phys. Soc. 16, 646 (1971); and to be published.
[18]H. R. Weller, Phys. Rev. Letters 28, 247 (1972).
[19]G. H. Rawitscher, Phys. Rev. C 6, 1212 (1972).
[20]P. E. Hodgson, *The Optical Model of Elastic Scattering* (Clarendon Press, Oxford, England, 1963), p. 58.

PHYSICAL REVIEW C VOLUME 7, NUMBER 2 FEBRUARY 1973

Study of ^{42}K, ^{42}Ca and ^{46}K, ^{46}Ca by Pickup Reactions

Y. Dupont,* P. Martin, and M. Chabre†
Institut des Sciences Nucléaires, BP n° 257, Centre de Tri, 38044 Grenoble, France
(Received 11 September 1972)

The ^{44,48}Ca$(p,t)^{42,46}$Ca and ^{43}Ca$(p,d)^{42}$Ca reactions have been investigated at 40 MeV, and the ^{44,48}Ca$(p,{}^3$He$)^{42,46}$K reactions at 40 and 56 MeV. Analysis of angular distributions leads to new spin assignments. Distorted-wave Born-approximation calculations are performed for (p,d) and (p,t) reactions. The nucleus ^{42}Ca being reached by both reactions, comparison is made between the results of calculations of the two processes. Potassium isotopes are studied through the comparison of analog states observed in the (p,t) reaction with the states reached in the $(p,{}^3$He) reaction. In the $(p,{}^3$He) spectra, the analogs of the ^{42}Ar and ^{46}Ar ground states have been identified.

I. INTRODUCTION

The calcium region has been the subject of numerous experimental investigations as well as extensive theoretical calculations.[1,2] However, only a few studies of the neutron states in the even isotopes through the two-neutron pickup reaction (p, t) have yet been published. In previous studies at comparatively low beam energies the analysis was restricted to the ground state and low-lying states due to lack of structure of the angular distributions.[3,4]

With a 40-MeV proton beam and good particle identification one can study states up to 15-MeV excitation energy in the residual nucleus. One then reaches the region of the analog states of the corresponding potassium isotopes. All angular distributions show enough structure to be characteristic of the L transfer; this allows unambiguous spin and parity assignments when starting from a doubly even target nucleus. The simultaneous study of the $(p,{}^3$He) reaction and the comparison of the ^{3}He spectra with the triton spectra in the analog-state region makes it possible to assign spin and parity to states in potassium isotopes that otherwise can be reached only by complex reactions.[5]

In this paper we present studies on the ^{42}Ca and ^{46}Ca isotopes; since analog states are observed in both nuclei this study was extended to the ^{42}K and ^{46}K isotopes.

The nucleus ^{42}Ca was reached in the ^{44}Ca$(p, t)^{42}$Ca reaction and in the one-nucleon-transfer reaction ^{43}Ca$(p, d)^{42}$Ca. The neutron-hole amplitudes obtained in the (p, d) reaction may be used to check the normalization of the distorted-wave Born-approximation (DWBA) calculation of the (p, t) reaction and also to resolve ambiguities in the (p, t) analysis. For negative-parity states one can determine this way the relative phases of the two components of a configuration mixing whose percentage has been obtained in the analysis of the (p, d) reaction. The combined results of these two reactions for positive-parity states give a sensitive test of the wave functions calculated by Gerace and Green.[6]

The nuclei ^{46}Ca and ^{46}K have been studied in the ^{48}Ca$(p, t)^{46}$Ca and ^{48}Ca$(p,{}^3$He$)^{46}$K reactions. Due to the lack of wave-function calculations for ^{46}Ca, the conclusions drawn from the DWBA analysis of the (p, t) reaction are mostly restricted to spin and parity assignments; but a lot of new information on the low-lying states of ^{46}K is obtained from the comparison of the (p, t) and